

## Tourmaline-rich pseudomorphs in sillimanite zone metapelites: Demarcation of an infiltration front

BARBARA L. DUTROW,<sup>1,\*</sup> C.T. FOSTER JR.,<sup>2</sup> AND DARRELL J. HENRY<sup>1</sup>

<sup>1</sup>Department of Geology and Geophysics, Louisiana State University, Baton Rouge, Louisiana 70803, U.S.A.

<sup>2</sup>Department of Geology, University of Iowa, Iowa City, Iowa 52242, U.S.A.

### ABSTRACT

Textural features combined with mineral chemistry preserved in metamorphic rocks provide insights into metamorphic reaction mechanisms as well as open vs. closed system processes. Prograde tourmaline-rich muscovite pseudomorphs after staurolite develop in sillimanite zone metapelites adjacent to peraluminous granitoid intrusives in NW Maine. Tourmalines occur in discrete domains restricted to central regions of muscovite-rich, quartz-poor pseudomorphs with biotite-rich margins. These tourmaline grains are relatively large (1.0 mm), lack detrital cores and exhibit only minor compositional zoning, in sharp contrast to matrix tourmaline from other samples. These features suggest fluid-infiltration as the causative mechanism for the formation of these tourmaline-rich mica pseudomorphs after staurolite.

Irreversible thermodynamic models of local reactions and material transport in combination with mineral chemistry allow evaluation of reaction mechanisms that produced these pseudomorphs. Thermodynamic models in the NCKMTFASHOB system mimic the observed textural features if a three-stage process is used. Stage 1: Staurolite replacement is initiated by infiltration of an aqueous phase that adds K+Na+H<sub>2</sub>O to the rock with the concomitant removal of Al+Fe. Because the system is initially undersaturated with respect to tourmaline, a pseudomorph containing muscovite with minor biotite develops at the expense of staurolite. Stage 2: With continued infiltration, concentration of B increases, tourmaline saturation is exceeded, tourmaline nucleates and grows. Local material transport constraints mandate that tourmaline precipitation be spatially restricted to regions of staurolite dissolution. Consequently, tourmaline forms in clusters at sites containing the last vestiges of staurolite in the pseudomorph core, also evidenced by staurolite inclusions within several tourmaline grains. Resultant domains of staurolite replacement during this stage contain about equal amounts of muscovite and tourmaline. Typical staurolite poikiloblast pseudomorphing reactions require silica transport, matrix quartz dissolves from the surrounding host resulting in a local enrichment of biotite and plagioclase at the pseudomorph margin. Stage 3: Small amounts of sillimanite nucleate and grow throughout the rock. Late-stage aqueous fluids from the adjacent monzonitic intrusive are likely to be the primary B source.

Theoretical, textural, and compositional modeling combined with observational data indicate that boron must have been derived externally from the rock, that the modal amount of tourmaline is very sensitive to the B content of the fluid, that tourmaline is stable throughout the sillimanite zone depending on other cation activities and pH of the fluid, and that these pseudomorphs provide insight into B contents of metamorphic fluids and the timing of the B influx. The outer geographic extent of the tourmaline-bearing pseudomorphs marks the boundary of a reactive geochemical front, and thus defines an advective isograd. Interpretation of subtle textural features preserved in the rock in conjunction with irreversible textural modeling provides a powerful tool with which to understand the chemical evolution of metamorphic rocks and the fluids involved.

### INTRODUCTION

Fluid infiltration accompanying metamorphism can profoundly influence the mineralogy, texture, and chemistry of the host rocks. As fluids move from one geochemical environment into another, fluids may advect chemical components that promote fluid-mineral reactions as the system moves back toward an equilibrium state. Evidence of these interactions is commonly

manifest in the residual bulk-rock chemistry, mineralogy, and textures. If metasomatism is extensive, obvious mineralogical evidence occurs in the form of skarns or metasomatic aureoles (e.g., Leeman and Sisson 1996). However, in some cases, effects are less dramatic, and only subtle textural and mineralogical features are recorded (e.g., Duke 1995). As such, mineralogy and textures may provide an important link between the controlling processes and the formation history of the rock. In addition, textures may provide evidence for migration of fluids in metamorphic terrains (c.f. Spear 1993, p. 677–687).

\*E-mail: dutrow@geol.lsu.edu

In metamorphic rocks, pseudomorphs and their associated mineral assemblages are especially useful in providing insights into the reaction history experienced by a terrane. Because pseudomorphing generally represents a local bulk compositional change, pseudomorphs preserve evidence of compositional evolution (e.g., Foster 1977). In addition, pseudomorphs are well suited to quantitative textural studies that permit their chemical evolution and formation to be deciphered. Previously, most quantitative textural studies have concentrated on closed system behavior (e.g., Foster 1981, 1990). However, textural analyses may also yield evidence of advective mass transport and fluid flow during metamorphism.

Although fluid infiltration during metamorphism has been described most commonly using major-element metasomatic and/or isotopic exchange arguments (e.g., Spear 1993; Ague 1994; Kohn and Valley 1994), mobile trace and minor elements may also provide crucial information about the movement of components during a metamorphic event. Boron is especially useful in metapelitic rocks because B is mobile in most aqueous fluids such that the fluids can act to enrich or disperse the element. Tourmaline requires B to form and, therefore, serves as an exceptional monitor of the availability and movement of B.

Most metamorphic tourmalines form from progressive release of B in a closed system, initially from fluids and clay minerals comprising the original sediments, and later from breakdown of micas (Henry and Dutrow 1992, 1996). Typically metamorphic tourmaline nucleates on preexisting detrital tourmaline cores and forms metamorphic overgrowths. This type of tourmaline growth is recognized easily, optically and chemically, by strong and discontinuous chemical, and commonly color, zoning that surrounds various detrital core compositions. Metamorphic tourmaline does not, however, require nucleation on detrital cores, and can form in their absence. Prograde metamorphic tourmalines without detrital cores also typically display discontinuous zoning that is formed during closed system growth. Alternatively, if the metamorphic system is open to fluid infiltration (i.e., open system) tourmaline may develop during a discrete stage when the metamorphic rock becomes locally enriched due to the influx of B-bearing fluids. In this case, the tourmaline is generally chemically homogeneous to very weakly zoned, and lacks the distinctive overgrowth patterns. For example, one type of tourmalinization is commonly observed in the country rocks near pegmatites where it is attributed to B-metasomatism and alkali leaching (e.g., Page et al. 1953; Shearer et al. 1984; Slack 1996). The original metamorphic assemblages are locally replaced by B-enriched assemblages, primarily tourmaline. This mineralogy is produced by a cation exchange mechanism due to the advection of components in the fluid. Tourmaline thus serves as a marker tracing movement of B in the system.

This paper reports on a very interesting textural and mineralogical feature, tourmaline-rich muscovite pseudomorphs after staurolite (Fig. 1), observed in sillimanite-bearing metapelites from west-central Maine. Field relations, mineral chemistry, and textural modeling studies of pseudomorphs constrain processes responsible for their formation, and establish their utility as infiltration monitors, recorders of mass transport attending metamorphism, and markers of an advective

isograd. In addition, this study provides insights into the composition of the local fluids infiltrating the country rock during Acadian metamorphism in NW Maine.

## GEOLOGIC SETTING

Samples utilized in this study were collected from metapelites adjacent to the North Jay Pluton, Farmington Quadrangle, west-central Maine (NJ in Figs. 2 and 3; Dutrow 1985). The metamorphic history of NW Maine is well documented (e.g., Holdaway et al. 1988; Guidotti 1970, 1989; Guidotti et al. 1996; De Yoreo et al. 1989), so only a brief synopsis of events relevant to these samples is presented here.

The Farmington area underwent multiple mid-Paleozoic metamorphic episodes (M1-M3) that were closely spaced in time and intensity (e.g., Holdaway et al. 1988; Guidotti and Holdaway 1993; Guidotti et al. 1998). Metamorphism attended the emplacement of numerous sheet-like intrusives of the Devonian New Hampshire Magma Series (e.g., Moench and Zartman 1976; Holdaway et al. 1982, 1988). Most intrusives are peraluminous quartz-monzonites containing biotite, muscovite, and garnet, in addition to potassium feldspar, plagioclase, and quartz. In most of this region, no more than two events can be recognized, M2 and M3, and are mappable as two clearly defined episodes. M2 is a widespread lower pressure event that produced andalusite-bearing assemblages. In the Farmington quadrangle, M2 is apparent only in the northwestern portion of the quadrangle, primarily recognized by retrograde chlorite-after-staurolite pseudomorphs that define a N-S trending isograd. This isograd is truncated by an E-W trending prograde M3 isograd in the southern half of the Farmington quadrangle (Fig. 2; Dutrow 1985; Holdaway et al. 1988; Guidotti and Holdaway 1993). The culmination of M3 in the southern portion of the Farmington area produced prograde garnet through sillimanite metamorphic zones. These obliterated much of the evidence for M2 in this region and retrogressed M2 assemblages to the north. Although M3 exhibits a regional character, isograds display a rough coincidence with exposed intrusive contacts. Intrusives are now exposed within the silli-

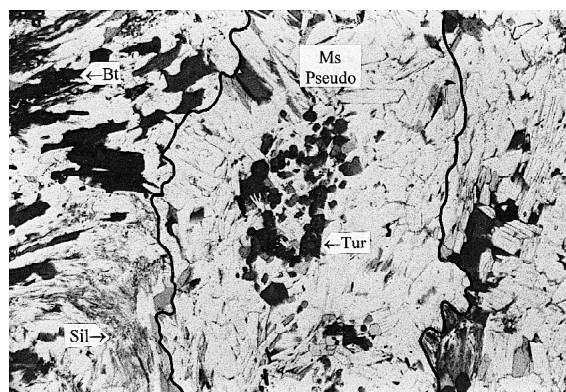


**FIGURE 1.** Photomicrograph of a tourmaline-bearing, muscovite-rich pseudomorph after staurolite that displays the change in grain size and mineral modes between matrix and pseudomorph; ms = light tabular grains within pseudomorph; bt = dark tabular grains; sil = gray needles. Dark line outlines pseudomorph. Note the clustering of tourmaline, dark grains, within the center of muscovite-rich area. (Field of view = 5.2 mm.)

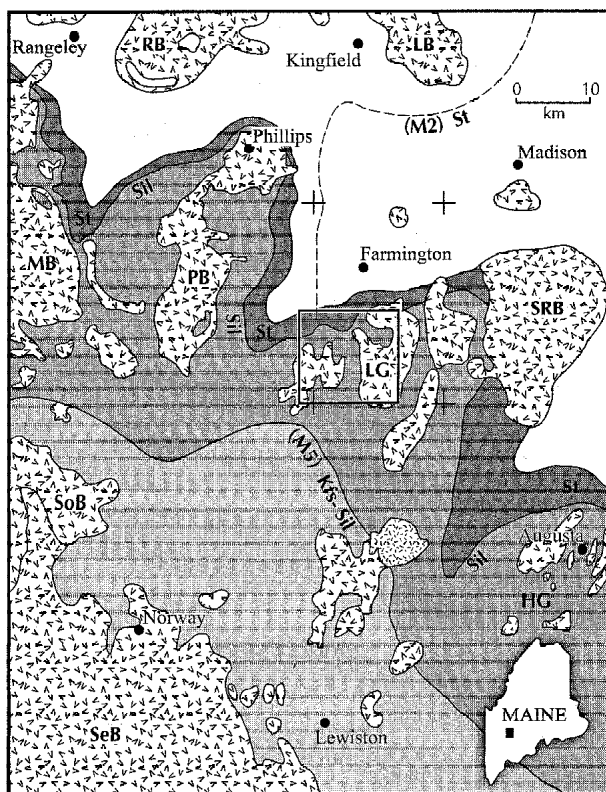


**FIGURE 2.** Generalized metamorphic map of NW Maine displaying M2 (dashed line), M3, and M5 metamorphic zones (adapted from Guidotti and Holdaway 1993). Grade of metamorphism decreases SW-NE and is noted by mineral abbreviations; Kfs-Sil (M5), Sil and St (M3), and St (M2). Gar and Chl zones are undifferentiated and to the north. Plutons are stippled and abbreviated: tourmaline-rich pseudomorphs are adjacent to: MB = Mooselookmeguntic and LG = Livermore Falls Group of which the North Jay pluton is a member. Location of the Farmington Quadrangle is bounded by crosses. Solid box is the study area shown in Figure 3. Cities are noted as landmarks.

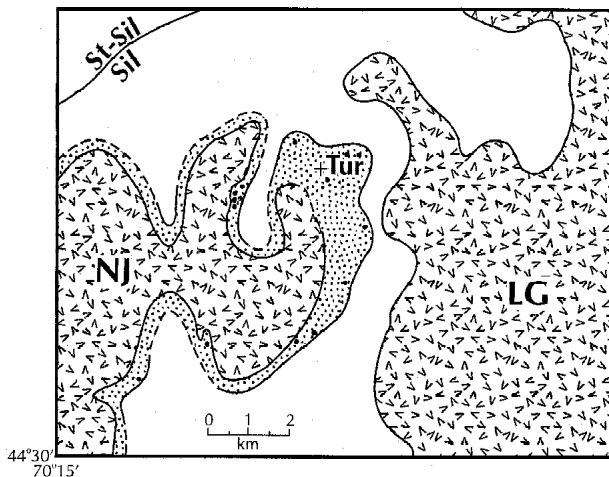


**FIGURE 3.** SW portion of the Farmington Quadrangle adjacent to the North Jay Pluton, NJ (see Fig. 2). Dots are locations of samples with tourmaline-rich muscovite pseudomorphs (after Dutrow 1985). "Tourmaline isograd" is outlined.

manite zone metamorphic rocks (Fig. 2).

Sangerville Formation metasediments comprise the dominant lithologic units that crop out in the Farmington area. The Sangerville is composed dominantly of eugeoclinal clastic and carbonate sediments of Silurian age (Moench and Pankiwskyj 1988). The units trend NE-SW and bedding in the metasediments intersects the intrusives at a high angle. Samples for this study were collected from all major units of the Sangerville, and are predominantly metapelitic.

Occurrence of the tourmaline-bearing muscovite pseudomorphs after staurolite defines a pattern roughly concentric to the peraluminous North Jay quartz monzonitic pluton (NJ, Fig. 3). Although genetically related plutons of the Livermore Falls Group (LG, Figs. 2 and 3) occur in the study area, glacial overburden and alluvial deposits from the Sandy Creek form a thick cover near pluton contacts that generally obscure the metapelitic host rocks. Consequently, the presence or absence of tourmaline-bearing assemblages associated with these plutons could not be confirmed and sample collection concentrated near the well-exposed North Jay pluton.

Pseudomorphs develop within the M3 sillimanite zone (Figs. 2 and 3). Temperature and pressure estimates, based on garnet-biotite geothermometry (Holdaway et al. 1997) and mineral stabilities (Dutrow 1985; Dutrow and Holdaway 1989), suggest that these samples formed at 575–600 °C and 3.25–3.5 kbar (see also Holdaway et al. 1988).

## DESCRIPTION OF TEXTURAL AND CHEMICAL FEATURES

### Analytical techniques

Microprobe analyses were carried out on four tourmaline-bearing rocks in order to characterize the samples chemically. Tourmaline and other silicates were analyzed quantitatively by wavelength-dispersive spectrometry (WDS) using the automated JEOL 733 electron microprobe at Louisiana State University. Analyses were done at an accelerating potential of 15 kV and a beam current of 5–10 nA using a 1–2  $\mu\text{m}$  focussed electron beam, except muscovite and biotite, for which a 10  $\mu\text{m}$  beam size was used. Well-characterized synthetic and natural silicates were used as standards. Data were corrected on-line using a modified Bence-Albee correction procedure. On the basis of replicate analyses of several secondary standards, analytical precision associated with counting statistics for selected oxides is estimated to be  $\pm 0.21\%$   $\text{SiO}_2$ ,  $\pm 0.13\%$   $\text{Al}_2\text{O}_3$ ,  $\pm 0.06\%$   $\text{FeO}$ ,  $\pm 0.11\%$   $\text{MgO}$ ,  $\pm 0.02\%$   $\text{CaO}$ , and  $\pm 0.03\%$   $\text{Na}_2\text{O}$ .

Tourmaline formulae were normalized on the basis of 15 cations exclusive of Na, Ca and K, which assumes no vacancies in the tetrahedral or octahedral sites and insignificant Li contents (see Henry and Dutrow 1996 for justification). The amount of  $\text{B}_2\text{O}_3$  necessary to produce three B cations in the structural formula was calculated from stoichiometric constraints (e.g., Hawthorne 1996; Bloodaxe et al. 1999)

### Sample description

Two types of sillimanite (sil) zone rocks (containing no potassium feldspar or staurolite) occur in the Farmington area. Both contain large muscovite-rich pseudomorphs after staurolite (e.g., "spangles" of Guidotti 1968), but are distinguished based on the presence or absence of tourmaline in the pseudo-

morph assemblage (e.g., Fig. 1). These sillimanite zone metapelites contain sillimanite (sil), muscovite (ms), biotite (bt), plagioclase (pl), ilmenite (ilm), quartz (qtz),  $\pm$  garnet (gar), graphite (gr), apatite (ap),  $\pm$  tourmaline (tur) (abbreviations after Kretz 1983). Staurolite (st) is present only as rare, small, isolated inclusions within three tourmaline grains. Potassium feldspar is not present.

### Pseudomorphs

Proximal to the pluton, large muscovite pseudomorphs after staurolite are abundant. Pseudomorphs are recognized by the marked increase in grain size of the pseudomorphing minerals as well as by the relative change in mineral modes from the pseudomorph to the matrix. Pseudomorphs, commonly up to centimeter size, are characterized by the predominance of coarse-grained muscovite ( $> 1.0$  mm), with small and variable amounts of biotite (Fig. 1). Minor quartz, sillimanite and traces of apatite are also present in some pseudomorphs. One pseudomorph contains abundant euhedral grains of apatite. Approximately 10% of the samples contain almandine-rich garnet within the pseudomorphs. Garnets display weak normal zoning as shown by a representative core-rim analyses (sample d167):  $\text{Alm}_{68.8}\text{Py}_{9.8}\text{Sp}_{18.0}\text{Gr}_{3.4}$  at the core to  $\text{Alm}_{71.7}\text{Py}_{8.9}\text{Sp}_{16.6}\text{Gr}_{2.8}$  at the inner rim (inner rim is defined as the zone not affected by late stage diffusion, see Holdaway et al. 1988). Garnet was not considered in the model calculations because it is absent in most pseudomorphs. Pseudomorphs retain the shape of the original staurolite, but staurolite has been totally replaced. These large muscovite segregations are readily apparent in hand specimen.

A striking feature of some pseudomorphs is anomalously high concentrations of tourmaline (up to  $\sim 30\%$ ) developed within, and confined to, the discrete domains of coarse-grained muscovite (Fig. 1). The abundant, relatively large tourmaline crystals, up to 1.0 mm, are typically clustered near the center of the pseudomorph. If tourmaline is present within the pseudomorph, it is generally absent from the matrix.

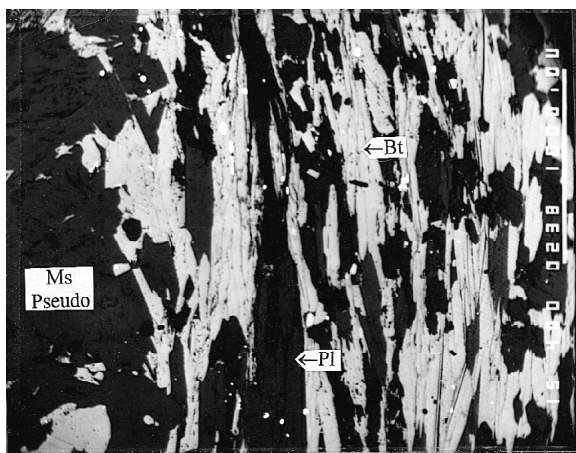


**FIGURE 4.** Backscattered electron image of the biotite (light gray) + plagioclase-rich mantle (dark-gray) surrounding the tourmaline-rich muscovite pseudomorph (dark gray, left side), as would be expected from calculations. (Sample d238, field of view = 0.3 mm.)

### Matrix

Matrix phases include  $\text{ms} + \text{bt} + \text{sil} + \text{pl} + \text{qtz} + \text{ilm} \pm \text{tur}$ , gr, gar, ap. Relative to the pseudomorph, there are lesser modal amounts of muscovite and tourmaline in the matrix but more biotite, sillimanite, plagioclase, quartz, and ilmenite (Fig. 1). The matrix-pseudomorph boundary is distinguished by a mantle region commonly enriched in biotite and plagioclase (e.g., Fig. 4) and depleted in quartz and muscovite relative to areas in the average matrix (Table 1), confirmed by X-ray mapping and image analyses. Although the absolute mineral modes vary among the samples, these trends are consistent among the different pseudomorph-bearing samples. Modal analyses of a representative pseudomorph sample and the adjoining regions illustrate these variations (Table 1). The compositions of muscovite and biotite are similar in both matrix and pseudomorph, as are compositions in the different samples (Table 2). Paragonite component in the muscovite ranged from 14.4–16.2%, typical of upper sillimanite zone compositions.

### Tourmaline

Tourmalines within the pseudomorphs are generally a uniform olive green color in transmitted light, rarely contain pale blue-green interiors, and have little or no color zoning. In a few cases, tourmalines have rims or patches with a brownish hue that corresponds to a small increase in Ti [ $0.02$  atoms per formula unit (apfu)]. The absence of significant color zoning correlates with the near constant chemical composition throughout the tourmaline, despite their relatively large size,  $> 1.0$  mm. For example, a detailed electron probe traverse of a 0.7 mm tourmaline (d241) reveals that  $\text{Mg}/(\text{Mg} + \text{Fe}_{\text{tot}})$  varies by only 0.063 from 0.526 to 0.588. Zoning due to undetected light elements such as Li is not probable, as Li contents in metapelitic tourmaline are typically low (e.g., Henry and Dutrow 1996). Compositionally, tourmalines within the pseudomorphs are aluminous schorl-dravites with  $\text{Mg}/(\text{Mg} + \text{Fe}_{\text{tot}})_{\text{rims}} = 0.57\text{--}0.60$  (Table 3). Systematic element partitioning between tourmaline rims and other ferromagnesium phases suggests that chemical equilibrium was approached (cf. Tables 2 and 3). Sillimanite inclusions within the tourmaline are common. Three of the tourmaline grains contain staurolite inclusions. The tourmalines are typically euhedral, displaying well-formed cross sections or prisms elongated parallel to c. One tourmaline grain displays evidence of resorption in the form of an embayed outline.

Two additional types of tourmaline occurrences are recognized in sillimanite zone samples that lack pseudomorphs as well as staurolite; (1) large ( $> 1$  mm), unzoned tourmaline dispersed throughout the matrix; and (2) small ( $< 0.3$  mm), zoned tourmaline that are developed within the matrix. These three

**TABLE 1.** Representative modal analyses for tur-pseudomorph samples

Sample no.	Mineral modes* (%)				
	Bt	Ms	Sil	Qtz + Pl	Tur
d245 Matrix	46.2	8.3	4.5	41.0	0.0
d245 Pseudo	8.6	64.9	11.2	4.9	10.4
d245 Mantle	66.1	2.7	7.1	24.1	0.0
d245 Avg. all regions	34.5	30.0	7.6	23.7	4.2

\* Based on 300 points for each region

**TABLE 2.** Representative chemical analyses of micas

Sample no.	Biotite			Muscovite		
	d167	d241	d245	d167	d241	d245
SiO <sub>2</sub>	35.44	34.91	34.52	45.32	45.43	45.12
Al <sub>2</sub> O <sub>3</sub>	19.31	19.23	19.31	35.71	36.02	36.13
TiO <sub>2</sub>	2.30	2.29	1.99	0.96	0.61	0.70
FeO	20.54	20.69	21.10	0.96	0.98	0.89
MnO	0.15	0.12	0.27	0.00	0.03	0.03
MgO	8.77	8.29	7.96	0.51	0.53	0.55
K <sub>2</sub> O	8.78	8.88	8.82	9.87	9.53	9.63
Na <sub>2</sub> O	0.23	0.30	0.29	1.20	1.21	1.07
BaO	n.d.	n.d.	n.d.	0.36	0.16	0.22
CaO	0.00	0.02	0.01	0.21	0.01	0.00
F	0.00	0.00	0.19	0.00	0.00	0.00
Total	95.52	94.73	94.46	95.10	94.51	94.34
O = F,Cl	0.00	0.00	0.08	00.00	0.00	0.00
<b>Formula proportions based on 22 O atoms</b>						
Si	5.389	5.371	5.355	6.057	6.079	6.052
<sup>IV</sup> Al	2.611	2.629	2.645	1.943	1.921	1.948
<sup>VI</sup> Al	0.850	0.858	0.885	3.682	3.759	3.763
Ti	0.263	0.265	0.232	0.096	0.061	0.071
Fe <sup>2+</sup>	2.612	2.662	2.737	0.107	0.110	0.100
Mn <sup>2+</sup>	0.019	0.016	0.035	0.000	0.003	0.003
Mg	1.988	1.901	1.841	0.102	0.106	0.110
<sup>VI</sup> tot	5.732	5.701	5.730	3.988	4.039	4.047
K	1.703	1.743	1.745	1.683	1.627	1.648
Na	0.068	0.089	0.087	0.311	0.314	0.278
Ba	n.d.	n.d.	n.d.	0.019	0.008	0.012
Ca	0.000	0.003	0.002	0.030	0.001	0.000
Alk <sub>(tot)</sub>	1.771	1.836	1.834	2.043	1.951	1.938
F	0.000	0.000	0.093	0.000	0.000	0.000
Mg/(Mg+Fe <sub>tot</sub> )	0.432	0.417	0.402	0.486	0.491	0.524

different types of tourmaline occurrences are systematically distributed around the intrusive at distinct distances from the contact. Samples with tourmaline-rich pseudomorphs are found closest to the contact, within 0.5–2 km of the pluton; followed by samples with large, unzoned tourmaline; and furthest from the contact are samples that contain small, zoned tourmaline that are typical of most metamorphic rocks.

### CHEMICAL AND TEXTURAL MODELING OF FLUID INFILTRATION

Muscovite-rich pseudomorphs after staurolite are a common prograde feature in many prograde metapelitic sequences. Previous work demonstrated that the initial stage of pseudomorph development takes place during closed-system prograde metamorphism when the upper thermal stability of staurolite is exceeded; muscovite replaces staurolite producing large coarse-grained muscovite-rich regions (e.g., Guidotti 1968; Foster 1977). These pseudomorphs after staurolite are found throughout sillimanite zone metapelites of Maine (e.g., Guidotti 1970) and are often termed “spangles” because they are easily observed in hand specimen. However, the development of tourmaline within these pseudomorphs appears to be unusual, with only one additional occurrence reported. Similar pseudomorphs were recognized in a core taken from lower sillimanite zone rocks adjacent to the peraluminous Mooselookmeguntic pluton, near Rangeley, Maine (Fig. 2; Loebner 1977).

The tourmaline-bearing pseudomorphs reported here are spatially restricted to the peraluminous North Jay monzonitic plu-

**TABLE 3.** Representative chemical analyses of tourmaline in pseudomorphs

Sample no.	Tourmaline		
	d167	d241	d245
B <sub>2</sub> O <sub>3</sub> *	10.36	10.68	10.63
SiO <sub>2</sub>	34.74	35.95	35.64
Al <sub>2</sub> O <sub>3</sub>	33.26	35.67	34.96
TiO <sub>2</sub>	0.88	0.78	0.87
Cr <sub>2</sub> O <sub>3</sub>	0.06	0.00	0.00
FeO	7.08	6.95	7.31
MnO	0.02	0.04	0.11
MgO	5.90	5.18	5.41
CaO	0.50	0.29	0.36
Na <sub>2</sub> O	1.92	1.92	1.95
K <sub>2</sub> O	0.04	0.03	0.04
F	0.00	0.00	0.18
Cl	0.00	0.00	0.00
Total	94.76	97.49	97.46
O = F,Cl	0.00	0.00	0.08
Total	94.76	97.49	97.39
<b>Formula proportions based on 15 cations (excluding K+Na+Ca+Ba)</b>			
B*	3.000	3.000	3.000
Si	5.830	5.852	5.826
<sup>VI</sup> Al	0.170	0.148	0.174
Al(Z)	6.000	6.000	6.000
Al(Y)	0.408	0.696	0.560
Ti	0.111	0.095	0.107
Cr	0.008	0.000	0.000
Fe <sup>2+</sup>	0.994	0.946	0.999
Mg	1.476	1.257	1.318
Y-site total	3.000	3.000	3.000
Ca	0.090	0.051	0.063
Na	0.625	0.606	0.618
K	0.009	0.006	0.008
X-site vacancy	0.277	0.337	0.311
F	0.000	0.000	0.093
Mg/(Mg+Fe <sub>tot</sub> )	0.598	0.571	0.569

\*B calculated by stoichiometry.

ton. The concentric distribution pattern cuts across major NE-SW-trending lithologic units of the Sangerville Formation (Fig. 3). Therefore, it does not appear that the tourmaline-pseudomorph samples are confined to a specific lithologic horizon.

The chemical homogeneity of tourmalines within the pseudomorphs suggests that the tourmaline developed during a discrete stage of B availability. This growth history is supported by comparison of pseudomorphous tourmaline with matrix tourmaline from other samples that lack the pseudomorphs and contain staurolite. Typical matrix tourmalines are small, 0.03 mm, may contain detrital tourmaline cores, and commonly exhibit sharp color discontinuities that correspond to abrupt chemical zonation. This growth pattern is interpreted to reflect compositionally distinct periods of metamorphic tourmaline growth, when B was available throughout the prograde metamorphic history of the system (Henry and Dutrow 1992, 1996). The chemical homogeneity of the pseudomorphous tourmaline cannot be attributed to homogenization due to volume diffusion at high temperature because, unlike most other minerals including garnet, tourmaline retains chemical zonation up to at least upper sillimanite zone conditions (Henry and Dutrow 1994, 1996).

The close spatial association of tourmaline-rich pseudomorphs with the intrusive, the chemical homogeneity of the relatively large pseudomorphic tourmaline, and the requirement of B to form tourmaline, strongly support a genetic relationship with the peraluminous pluton such that the intrusive may have supplied much of the B required for tourmaline development. Many alteration processes are driven by the transport of chemical components by a fluid derived from, or in equilibrium with, an intrusive (e.g., London et al. 1996). Boron can be highly mobile in aqueous fluids and the infiltration of B-bearing aqueous fluids from the adjacent pluton is a likely causative factor in the formation of these tourmaline-bearing pseudomorphs.

To evaluate fluid infiltration as a causative factor in tourmaline pseudomorph formation, the reactions responsible for the formation of the pseudomorphs and the metamorphic history imbedded in their textures, two approaches were taken. First, the relative stability of tourmaline with respect to cation fluid compositions was established using equilibrium activity diagrams to depict mineral phase relations as a function of aqueous ion activities. Second, irreversible thermodynamic modeling of mineral textures was utilized to determine the mineral reactions and material transport responsible for the pseudomorph formation.

#### Activity diagrams and cation fluid composition

Infiltration of fluids as a driving force for metamorphic reactions is well documented for metacarbonates (e.g., Ferry 1994). Typically, fluid compositions in metamorphic systems are described with respect to the volatile components  $H_2O$  and  $CO_2$ , to a lesser extent  $CH_4$ , without considering the cation compositions of the fluid phase.

However, infiltration of chemically distinct fluids with respect to the cation concentrations also drives mineral reactions. As fluid moves from its upstream region into the local environment, fluids may be out of equilibrium with the rocks that they infiltrated. Fluid-rock reactions are promoted as the system returns to equilibrium conditions (e.g., Norton 1987). Activity diagrams are useful guides to such reactions because they depict the ion activity ratios of the aqueous fluid phase in equilibrium with the coexisting minerals (e.g., Helgeson 1970; Bowers et al. 1984; Johnson and Norton 1985). The results of infiltration of compositionally distinct fluids can be visualized and evaluated easily, as fluid-rock reactions ensue.

The chemical system  $NaO-K_2O-MgO-FeO-Al_2O_3-SiO_2-B_2O_3-H_2O$  closely approximates the tourmaline-bearing pseudomorph assemblage. Textural, compositional, geothermometric and thermochemical data for minerals and fluids in this system were utilized to construct equilibrium activity diagrams that represent mineral phase relations in the sillimanite zone metapelitic rocks as a function of aqueous ion activity ratios (Dutrow et al. 1989; Dutrow and Foster 1992). Fluid-mineral phase boundaries are defined by equilibrium constants for hydrolysis reactions of stable phases found in the pseudomorph assemblage; tourmaline, muscovite, biotite, sillimanite, albite, quartz, and  $H_2O$ .

Equilibrium activity diagrams were calculated based on internally consistent thermodynamic data for minerals and aqueous species and complexes using SUPCRT92 (Johnson et al. 1992), with  $H_2O$  fluid properties from Johnson and Norton

(1991). Thermochemical data for tourmaline, consistent with this data base, were retrieved from experiments of Kuyunko et al. (1984). These diagrams use actual chemical compositions of the major mineral phases (Table 4; cf. Lynch and Ortega 1997) and include appropriate adjustments to the thermochemical data for binary Fe-Mg solid-solution in tourmaline (draviteschorl) and biotite and Na-K in the muscovite.

Because of the multicomponent nature of the chemical system, selected components must be explicitly assigned a value to reduce the system to two variables represented on the axes. These assigned values were based on constraints from natural assemblages. Fluids in equilibrium with metapelites are typically  $H_2O$ -rich. As such, a unit activity of  $H_2O$  was assumed. Coexisting quartz indicates that  $SiO_{2(aq)}$  is fixed at quartz saturation. Aluminum is chosen as the balancing component and, therefore, is conserved among the minerals; the value is fixed by the phases such that variations occur across the diagram. Calculation of log K values for various B complexes indicates that  $B(OH)_3$  is the stable B complex at these conditions (e.g., Bassett 1980; Shock et al. 1989) and was used as the B aqueous species. Limiting conditions for  $a_{B(OH)_3}$  in the fluid was estimated by assuming that the infiltrating fluid derived from, and was initially in equilibrium with, the adjacent peraluminous granitoid. Equilibrium values for aqueous ion activities in the pluton are constrained by the phases  $ksp + ab + bt + ms + gar + qtz$ , and the absence of tourmaline. Log activity values defined by this assemblage at 3.25 kbar and 700 °C, approximate conditions for pluton solidification, coupled with the log K for the tourmaline hydrolysis reaction, yield a maximum value for log  $[a_{B(OH)_3}]$  in the intrusive (e.g., that value of log  $[a_{B(OH)_3}]$  where tourmaline becomes stable with the pluton assemblage). This value also determines the initial maximal B activity for infiltration of the country rocks. Values for the activity ratios of Fe and K in the aqueous fluids were constrained by the equilibrium assemblage present in most pseudomorphs,  $ms + tur + sil$ , such that the correct assemblage and topology of the diagram was produced.

A representative activity diagram for fluids in equilibrium with tourmaline-bearing pseudomorphs, at the estimated pressure and temperature of the sillimanite zone, is shown in Figure 5 as a function of the variables log  $(a_{Na^+}/a_{H^+})$  and log  $(a_{Mg^{2+}}/a_{H^+}^2)$ , assuming quartz saturation, a unit activity of  $H_2O$ , and the estimated values of log  $(a_{K^+}/a_{H^+})$ , log  $(a_{Fe^{2+}}/a_{H^+}^2)$ , and log  $[a_{B(OH)_3}]$ . Increasing  $(a_{Na^+}/a_{H^+})$  stabilizes sillimanite, muscovite and then albite. As  $(a_{Mg^{2+}}/a_{H^+}^2)$  increases, biotite is stabilized relative to sillimanite. If staurolite is present, a small staurolite field bisects the sillimanite and biotite fields. Tourmaline is stable at intermediate values of log  $(a_{Na^+}/a_{H^+})$  and log  $(a_{Mg^{2+}}/a_{H^+}^2)$ . Two fields of tourmaline stability are displayed as a function of  $a_{B(OH)_3}$ . At log  $[a_{B(OH)_3}] = -11.0$ , tourmaline disappears and is replaced by albite, muscovite and biotite (Fig. 5). Increasing only  $a_{B(OH)_3}$  dramatically increases the stability field for tourmaline with respect to the activity ratios of Na and Mg. At log  $[a_{B(OH)_3}] = -10.5$ , the tourmaline field intersects  $ab + ms + bt$  fields. Additional increases in  $a_{B(OH)_3}$ , holding other variables constant, cause the tourmaline field to expand further, intersecting the sillimanite field. These estimated values of log  $[a_{B(OH)_3}]$  produce the correct phase topology for the observed

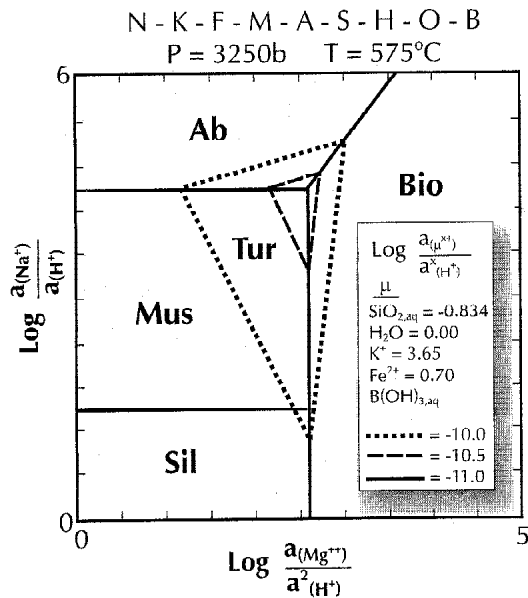


**FIGURE 5.** Equilibrium activity diagram for the NKFMAHOB system. Diagram is constructed for quartz saturation,  $a_{\text{H}_2\text{O}} = 1.0$ , and values given. Mineral compositions utilized are from electron probe analyses with thermodynamic data corrected for composition. Different values of  $\text{B(OH)}_3$  display expansion of tourmaline stability field with increasing B activity. Note that at  $\log [a_{\text{B(OH)}_3}] = -11$ , tourmaline is not stable at these conditions (solid lines) and is replaced by  $\text{ab} + \text{sil} + \text{ms}$ .

assemblage of coexisting  $\text{ms} + \text{sil} + \text{tur}$  for the estimated conditions. These data imply that the minimum  $\log [a_{\text{B(OH)}_3}]$  required to produce the tourmaline pseudomorphs was about  $-10.5$ , the  $\log (a_{\text{Mg}^{2+}}/a_{\text{H}^+}^2)$  was about  $2.5$  and the  $\log (a_{\text{Na}^+}/a_{\text{H}^+})$  was in the vicinity of  $3.5$ . Slightly lower  $a_{\text{B(OH)}_3}$  values and higher  $(a_{\text{K}^+}/a_{\text{H}^+})$  values promote the assemblage  $\text{tur} + \text{ms} + \text{bt} + \text{sil} (+\text{qtz} + \text{H}_2\text{O})$  such that small fluctuations in activities of B and K produce assemblages containing both micas, an assemblage observed in some pseudomorphs. To produce  $\text{tur} + \text{sil} + \text{bt}$  from  $\text{ms} + \text{sil} + \text{bt} + \text{st}$ , at constant  $T, P$ , and constant B and quartz activities,  $(a_{\text{K}^+}/a_{\text{H}^+})$ ,  $(a_{\text{Mg}^{2+}}/a_{\text{H}^+}^2)$  must decrease whereas  $(a_{\text{Fe}^{2+}}/a_{\text{H}^+}^2)$  must increase in the fluid. This is achieved by dissolution of staurolite, increasing Fe, and precipitation of muscovite and tourmaline, resulting in decreased K and Mg in the fluid.

These limiting data can be combined with experiments of tourmaline stability in the  $\text{tur} + \text{bt} + \text{ab}$  system (Morgan and London 1989) to determine approximate activities of cation species. Experiments indicate that fluids must have  $\text{pH} < 5.5$ – $6.0$  for tourmaline to be stable in this system. Assuming  $\text{pH} = 4.0$ , activities of the cations are:  $a_{\text{Na}^+} = 0.56$ ,  $a_{\text{K}^+} = 0.45$ ,  $a_{\text{Fe}^{2+}} = 5e^{-8}$ , and  $a_{\text{Mg}^{2+}} = 3.5e^{-6}$ . The presence of significant quantities of apatite within one pseudomorph suggests an increase in the activity of P and F late in the pseudomorphing process.

The widespread occurrence of tourmaline in sillimanite zone rocks also demonstrates that tourmaline is stable at relatively high metamorphic grade. However, cation fluid compositions may exert a fundamental control on tourmaline stability. As  $(a_{\text{Na}^+}/a_{\text{H}^+})$  increases, tourmaline is stabilized over biotite plus sillimanite (Fig. 5). Consequently, the occurrence of  $\text{bt} + \text{sil}$  without tourmaline could also be due to lower  $\log (a_{\text{Na}^+}/a_{\text{H}^+})$  and  $(a_{\text{Fe}^{2+}}/a_{\text{H}^+}^2)$

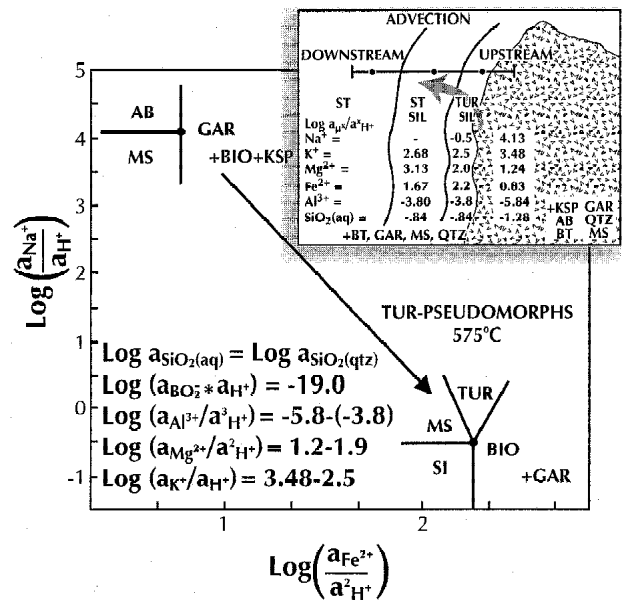


**FIGURE 6.** Representative cation compositions of fluid in equilibrium with pluton and with tourmaline-rich pseudomorphs. Fluids are out of equilibrium downstream (tur zone), which causes advection of components and fluid-mineral interactions resulting in the formation of tourmaline-rich pseudomorphs. The flux of components necessary is given by the change in activity ratios over the distance from the pluton to the pseudomorphs.

and may not reflect the upper thermal stability of tourmaline, as is commonly assumed. These data also suggest that the concentration of the cation constituents in the fluid phase, as well as B, have a dominating influence on the occurrence of tourmaline at high-grade metamorphic conditions (Fig. 5).

Fluid cation concentrations can also explain the notable paucity of matrix tourmaline in samples that display tourmaline-rich pseudomorphs. These contrast with staurolite or other sillimanite zone samples that lack tourmaline-rich pseudomorphs and contain matrix tourmaline. Infiltration of an early compositionally distinct fluid, out of equilibrium with matrix tourmaline, may dissolve this tourmaline and reprecipitate the constituents as a subordinate amount of tourmaline within the pseudomorph (see below). For example, fluids in equilibrium with the intrusive contain higher activities of Na, K and lower Al, Mg, and Fe than fluids in equilibrium with the metapelitic pseudomorph mineral assemblage (Fig. 6). This difference in activities represents the driving force for the chemical reaction that must occur to attain equilibrium values between the metapelitic assemblage and the fluid.

Mineral assemblages preserved as pseudomorphs help constrain cation compositions of the infiltrating fluid. Because tourmaline requires B to form, these pseudomorphs potentially provide insights into B contents of metamorphic fluids as well as the processes required for their formation and the timing of B flux.

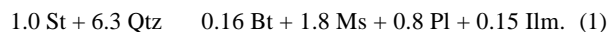
### Textural modeling

Mineral reactions likely to be responsible for the formation of the tourmaline-rich pseudomorphs after staurolite (Fig. 1) were investigated with irreversible thermodynamic models of local re-

actions and material transport using the textural modeling program SEG (Foster 1993) after the method of Fisher (1975, 1977). This approach combines material transport equations, conservation equations, and Gibbs-Duhem equations at constant  $T$  and  $P$  to calculate reaction mechanisms that develop in a rock under conditions of local equilibrium (Foster 1981), with constraints from natural samples. Mineral compositions utilized for modeling were determined from electron microprobe analyses (Table 4; cf. Tables 2 and 3); Mn was minor and not considered. Mineral modes were estimated from thin sections (e.g., Table 1), X-ray mapping, and image analyses. Relative diffusion coefficients were taken from Foster (1981), with the exception of those for B and  $\text{SiO}_2$ , which are estimated in this study.

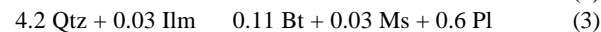
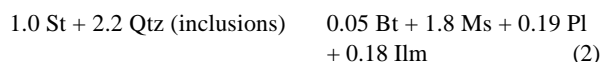
The above observations and analyses suggest that the pseudomorphs develop in a system open to an infiltrating fluid that serves as a source/sink for components consumed/produced by the pseudomorphing reactions. The fluid appears to provide K (see previous discussion) because sillimanite, that normally forms from the Al liberated by staurolite breakdown, is much lower in abundance than the amount expected to develop in a closed system. Instead, the Al produced by staurolite breakdown is consumed by micas formed as a result of K metasomatism. In addition, the infiltrating fluid was also assumed to be low in B initially but higher in B later because the concentration of tourmaline in the pseudomorph center (Fig. 1) suggests that tourmaline growth began after staurolite had been already partially pseudomorphed by micas. The dissolving staurolites were assumed to communicate with the infiltrating fluid reservoir by diffusion because the presence of biotite + plagioclase-rich mantles around the pseudomorphs (e.g., Figs. 1 and 4; Table 1) indicates that material transport to local reaction sites was diffusion controlled.

To produce the textural features similar to those observed, a three-stage pseudomorphing process is required in which the rock is open to fluids, at least at the hand-specimen scale. The initial conditions for the calculations consisted of a typical staurolite zone metapelite: poikiloblastic staurolites with 10% quartz inclusions set in a matrix of 54% quartz, 20% biotite, 20% muscovite, 5% plagioclase, and 1% ilmenite (Fig. 7a). When staurolite begins to dissolve in the rock, material transport constraints imposed by local equilibrium with the matrix phases results in the following reaction between the staurolite and the matrix:



Constituents to balance this reaction are transported through the matrix by diffusion under local equilibrium conditions. Na,

Ca, K, Ti, and  $\text{H}_2\text{O}$  are supplied to reaction 1, where they are consumed. Fe, Mg, and Al are produced by reaction 1 and transported away from the reaction site by diffusion through the matrix. This reaction consumes stqtz in a volumetric ratio of about 3:1. Staurolite poikiloblasts with more than 24% quartz inclusions will have sufficient quartz in the poikiloblast to supply the necessary  $\text{SiO}_2$  required for the reaction. These quartz-rich poikiloblasts are replaced by a muscovite-rich pseudomorph that also contains biotite, plagioclase, ilmenite and any excess quartz not consumed by reaction 1 (Foster 1981). Poikiloblasts with <24% quartz do not contain sufficient quartz to balance reaction 1. For example, a poikiloblast with 10% quartz inclusions (Fig. 7a) requires about half of the  $\text{SiO}_2$  needed for reaction 1 to be derived from quartz in the surrounding matrix. This causes reaction 1 to proceed via two reactions, one that consumes the staurolite poikiloblast (reaction 2) and one that consumes matrix (reaction 3):



The stoichiometry of reactions 2 and 3 depends upon the value of the Si diffusion coefficient, which could not be determined by Foster (1981) because rocks in that study were all quartz-bearing. The value of the Si diffusion coefficient used here is six times that of K, which results in pseudomorphs with a small amount of biotite (Fig. 7b), as observed in these samples (Fig. 1). Lower values for the Si diffusion coefficient produce pseudomorphs containing no biotite, and higher values produce too much biotite in the pseudomorph when compared with natural samples. Reaction 3 consumes matrix quartz and produces a distinct biotite and plagioclase-rich mantle at the margin of the pseudomorph, a feature confirmed by backscattered electron imaging and image analysis, of several samples (Fig. 4). The thickness of this mantle depends on the amount of poikiloblastic quartz available in the staurolite vs. that required from the matrix. Poikiloblasts with few quartz inclusions have prominent biotite + plagioclase mantles, whereas those with abundant quartz have biotite + plagioclase mantles that are thin or absent.

The sum of the local reactions that create the staurolite pseudomorph produces Fe, Mg, and Al while consuming Na, K, Ca, and Ti. These components are supplied or removed by diffusional transport through the matrix around the staurolite. In typical sillimanite zone rocks, components produced/consumed by the staurolite-pseudomorphing reactions are consumed/produced by local reactions growing sillimanite elsewhere in the rock, so that the overall reaction is balanced at the whole rock scale for all components except  $\text{H}_2\text{O}$ , which migrates out of the rock (Foster 1977, 1981, 1983). Rocks with abundant tourmaline in the pseudomorphs typically do not have sufficient sillimanite to balance the components produced or consumed by the staurolite-pseudomorphing reactions, indicating they were open to infiltrating fluids with K. Model calculations for the rock (Figs. 7a–d) assume that all the constituents transported through the matrix around dissolving staurolites had an infiltrating fluid that acted as a source or sink at the hand-specimen scale such that no sillimanite was

**TABLE 4.** Idealized composition of minerals used for textural modeling

	N - K - C - F - M - T - A - S - H - O - B System
Tur	$\text{Na}_{0.58} \text{Ca}_{0.06} \text{Fe}_{0.99} \text{Mg}_{1.29} \text{Al}_{6.80} \text{Ti}_{0.08} (\text{BO}_3)_3 \text{Si}_{5.73} \text{O}_{18} (\text{OH})_4$
Bt	$\text{K}_{1.75} \text{Na}_{0.07} \text{Fe}_{2.73} \text{Mg}_{1.83} \text{Ti}_{0.29} \text{Al}_{3.48} \text{Si}_{5.35} \text{O}_{20} (\text{OH})_4$
Ms	$\text{K}_{1.64} \text{Na}_{0.31} \text{Al}_{5.78} \text{Fe}_{0.11} \text{Mg}_{0.10} \text{Ti}_{0.06} \text{Si}_6 \text{O}_{20} (\text{OH})_4$
St	$\text{Fe}_{3.37} \text{Mg}_{0.57} \text{Al}_{17.81} \text{Ti}_{0.12} \text{Si}_{17.62} \text{O}_{48} \text{H}_{3-38}$
Gar	$\text{Fe}_{2.17} \text{Mg}_{0.25} \text{Ca}_{0.07} \text{Al}_{2.01} \text{Si}_{3.0} \text{O}_{12}$
Pl	$\text{Na}_{0.78} \text{Ca}_{0.21} \text{K}_{0.03} \text{Al}_{1.23} \text{Si}_{2.77} \text{O}_8$
Ilm	$\text{Fe}_{1.96} \text{Ti}_{2.02} \text{O}_6$
Sil	$\text{Al}_2 \text{Si O}_5$
Qtz	$\text{Si O}_2$

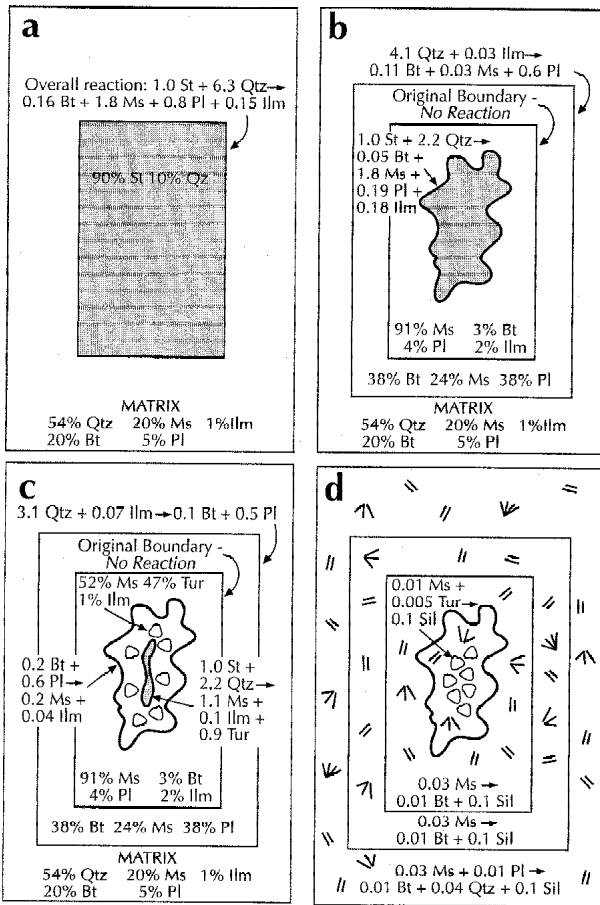
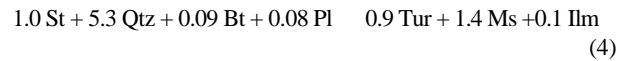


**FIGURE 7.** (a) Starting configuration for texture models showing overall reaction at the beginning of staurolite dissolution. Note that the volume proportion of quartz to staurolite in the poikiloblast (1:3) is lower than the volume proportion used by the overall reaction, requiring some quartz to be provided by dissolution of the matrix. (b) Staurolite dissolution prior to tourmaline saturation, which produces a muscovite-rich pseudomorph with minor amounts of biotite, plagioclase, and ilmenite. Note the plagioclase and biotite-rich, quartz-free mantle around the pseudomorph is produced by consumption of quartz in the matrix (see Fig. 4). Components to balance overall reaction diffuse through matrix to infiltrating fluid pathways, which serve as a metasomatic source/sink at the hand specimen scale. (c) Tourmaline saturation with continued staurolite dissolution. Although tourmaline was allowed to nucleate throughout the rock, most tourmaline growth takes place at the site of staurolite dissolution. Boron for tourmaline growth is provided by the infiltrating fluid and diffuses through the matrix from fluid pathways to the reaction sites. (d) Late sillimanite nucleation and growth throughout the rock (cf. Fig. 1).

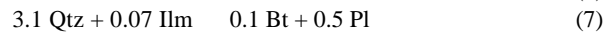
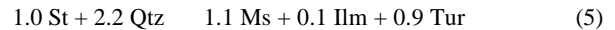
produced in the rock. Natural samples display a continuous range of sillimanite modes from specimens with abundant staurolite pseudomorphs and virtually no sillimanite, to specimens with exactly the amount of sillimanite required to balance the staurolite breakdown reaction. This indicates that the amount of metasomatism varies from sample to sample. The fluid acting as a source or sink for components in these early pseudomorphs was probably undersaturated with respect to tourmaline, causing pre-existing tourmalines to dissolve. This range in sil-

limanite modes accounts for the absence of tourmaline with detrital cores in rocks that contained tourmaline pseudomorphs in this study. The small amounts of B liberated from these dissolved tourmalines are insufficient to raise the amount of B in the early fluids to the level required for equilibration with tourmaline. Consequently, all the detrital tourmalines are dissolved by the early fluid and the addition of B from an external source is required to re-saturate the rock with respect to tourmaline.

The second stage of pseudomorph development was modeled by allowing tourmaline to nucleate throughout the rock due to increasing B concentration in the infiltrating fluid (Fig. 7c), which is thought to represent fluids from the cooling North Jay pluton. As in the first stage, the local reactions that develop communicated with the infiltrating fluid pathways via diffusive transport through the matrix. When tourmaline is added to the assemblage, the overall reaction that dissolves the remaining staurolite is:



The poikiloblastic staurolite contains less quartz than consumed by this reaction, and no biotite or plagioclase, so the reaction will split into three parts, one that consumes staurolite (reaction 5) one that consumes biotite and plagioclase in the earlier-formed pseudomorph (reaction 6), and one that consumes matrix quartz (reaction 7):



The pseudomorph produced by this reaction mechanism is shown in Figure 7c. Note that the outer portion of the pseudomorph and inner part of the biotite + plagioclase-rich mantle (Fig. 4) were produced prior to tourmaline saturation (Fig. 7b). The amount of tourmaline produced by reaction 5 depends upon the value of the B diffusion coefficient. When the B diffusion coefficient equals the K diffusion coefficient a volume of tourmaline is produced that is half the amount of muscovite produced. This appears to be slightly lower than the proportions observed in these samples. Consequently, the value for the B diffusion coefficient used to calculate Figure 7c is twice the value of the K diffusion coefficient. This value produces nearly equal proportions of tourmaline and muscovite in the pseudomorph core, similar to that observed in natural samples (Fig. 1). Increasing the B diffusion coefficient further results in substantially higher proportions of tourmaline in the pseudomorph. This is a situation analogous to tourmalinization. Although the entire rock is saturated with tourmaline nuclei, tourmaline production is located at the site of the staurolite dissolution reaction, which supplies essential components (Al, Fe, Mg) for growth of tourmaline. This reaction mechanism is supported by the presence of staurolite inclusions within some tourmaline. A cluster of tourmalines form within the pseudomorph interior, as observed (Fig. 1).

The third stage of pseudomorph development is the nucleation and growth of small amounts of sillimanite throughout

the rock (Figs. 1 and 7d). The local reactions were calculated by allowing sillimanite to grow in three locations where it is typically observed in natural specimens. (1) The center of the pseudomorph and the biotite-plagioclase-rich mantle, where material transport to the reaction site is constrained by local equilibrium with tourmaline, ilmenite, and muscovite. (2) The outer portion of the pseudomorph, where material transport is constrained by local equilibrium with muscovite, biotite, plagioclase and ilmenite. (3) The matrix, where material transport is constrained by local equilibrium with muscovite + biotite + plagioclase + ilmenite + quartz. The model texture (Fig. 7d) matches the features observed in many tourmaline-rich rocks where small amounts of sillimanite grew at the expense of all of the earlier-formed features. This may explain the embayments noted in some tourmalines. However, there are other samples where some sillimanite growth appears to be simultaneous with the early stage pseudomorphing reactions, apparently because the infiltrating fluids did not supply sufficient K to eliminate sillimanite production. Textures in these rocks represent a hybrid between those shown in Figures 7b–d and the textures discussed by Foster (1977, 1981). When tourmaline nucleates and grows in rocks with early sillimanite, it can grow at the expense of sillimanite by a reaction that is the reverse of the reaction involving tourmaline shown in Fig. 7d.

This analysis demonstrates that reaction mechanisms are controlled by a process involving infiltration of a fluid that serves as a source and sink for the components required by local reactions to produce tourmaline-rich pseudomorphs similar to those observed (Fig. 1). In the early stage of infiltration, the fluid provides a source of K that causes Al produced by the staurolite breakdown reaction to be converted to micas instead of sillimanite (Fig. 7b). The early fluid is also undersaturated with respect to tourmaline, causing pre-existing tourmaline to dissolve. As infiltration continues, B in the fluid increases to values that saturate the grain boundary fluid in the rock with respect to tourmaline, and tourmaline begins to grow as staurolite progressively dissolves (Fig. 7c). Although tourmaline is saturated throughout the rock, material transport constraints force tourmaline growth to be concentrated in clusters in the pseudomorph core where sufficient nutrients from the remaining staurolite exist. The amount of tourmaline formed is sensitive to the availability of B in the infiltrating fluid and the amount of staurolite remaining to be dissolved when tourmaline becomes stable in the rock. These types of textures can be produced by influx of H<sub>2</sub>O-rich fluids containing relatively small concentrations of B. As such, they provide an indication of the B content of the fluid. Similar reaction mechanisms can form tourmaline at the expense of sillimanite in rocks where the supply of K in the early stages of infiltration is not sufficient to convert the Al produced by staurolite breakdown to micas, allowing early sillimanite to form prior to saturation with tourmaline. Subsequent nucleation of tourmaline near sillimanite will grow tourmaline at the expense of sillimanite.

## DISCUSSION

Textural modeling studies presented here suggest that formation of the high modal amounts of tourmaline within the pseudomorphs require an externally derived aqueous fluid that

was relatively enriched in B, and to a lesser extent, K. In addition, the chemical homogeneity of the tourmalines indicates that their formation occurred in a uniform chemical environment when B was made available to the system. The most likely source of the B-bearing fluid was the adjacent peraluminous granitic intrusive, as demonstrated by the spatially restricted, concentric distribution pattern of the tourmaline-bearing pseudomorphs proximal to the pluton.

Boron-rich pneumatolytic aqueous fluids infiltrating the surrounding metapelites from the adjacent granitic source is likely for several reasons. (1) Fluids derived from granitic-pegmatitic systems can exhibit strong B enrichments, up to 10 wt% B<sub>2</sub>O<sub>3</sub> (e.g., London 1986). Thus, exsolved H<sub>2</sub>O-rich fluids derived from granitic rocks provide an effective transport medium for B (e.g., London et al. 1988). (2) Boron is highly mobile and easily leached and redistributed especially under alkaline pH conditions (e.g., Bassett 1980; Shaw et al. 1988; Dingwell et al. 1996; Henry and Dutrow 1996). (3) Hydrogen isotope investigations of mica from nearby sillimanite zone metapelites corroborate that there was extensive fluid infiltration from granitic intrusives in the region (Colucci et al. 1991). (4) With increasing distance from the pluton, the tourmaline present within the metapelites reverts to the typical prograde, highly zoned tourmaline that may contain detrital cores. It does not appear that the B required for tourmaline formation was derived in a closed system from preexisting matrix tourmaline, because matrix tourmaline is not sufficiently abundant to supply the required B for the modal amounts of tourmaline observed in the pseudomorphs. (5) Studies indicate that the average modal amount of tourmaline in amphibolite facies metapelites is approximately 0.3% (which translates to approximately 97.8 ppm B for the average rock), and that the amount of B fixed in tourmaline comprises an increasingly greater proportion of whole-rock B with increasing grade (up to 70% in amphibolite facies metapelites; Sperlich et al. 1996). If this is the case, these high-grade rocks have most of the B tied up in tourmaline. Our modal estimate is ~3%, which translates to almost 1000 ppm B. This is high for any pelitic sediment and argues for the necessity for the external input of B.

Furthermore, and more obvious, evidence for B-rich fluid infiltration from a magmatic source derives from tourmaline-bearing contact aureoles that are observed to surround many igneous intrusives (e.g., Leeman and Sisson 1996). These aureoles are attributed to metasomatic processes relating to magma crystallization. In situations where late stage hydrothermal/magmatic fluids are extremely enriched in B, tourmalinites may form (e.g., Slack 1996); tourmalinites are rocks that also mark the extent of chemically reactive fluids. Slack (1996) proposes that one type of tourmalinite may form from B-enriched fluids released during amphibolite-grade metamorphism. Data from the present study suggests, however, that B will be trapped during amphibolite grade metamorphism if sufficient components (e.g., Na, Al, and Fe) are present to form tourmaline and the pH of the fluid is sufficiently low.

If fluids were initially in equilibrium with the pluton, the upstream condition (Norton 1988), they would be out of equilibrium as they infiltrated the lower sillimanite zone metapelites, the downstream condition (Fig. 6). Infiltration of chemically

distinct fluids provides a driving force for chemical reactions as the fluids attain equilibrium. These fluid-mineral reactions involve the precipitation of tourmaline within the muscovite-rich pseudomorphs as Al, Fe, and B in the fluid increase to values that saturate the local environment with respect to tourmaline. Consequently, the zone of tourmaline-rich, pseudomorph-bearing rocks represents a front of geochemical activity where upstream fluids have attained equilibrium with downstream rock compositions. The outer extent of the tourmaline-rich pseudomorphs marks the reaction zone and the limit of a chemically reactive infiltration front. As such, this boundary defines an "advective" isograd (e.g., Dutrow and Norton 1989).

Advective fronts are well documented for fluid infiltration in metacarbonates interbedded with metapelites (e.g., Bickle and Baker 1990). Infiltration of dramatically different H<sub>2</sub>O vs. CO<sub>2</sub> fluid compositions into host rocks, causes a specific sequence of mineral assemblages to form (e.g., Greenwood 1975; Rice and Ferry 1977; Ferry 1991 and references therein), and/or stable isotopic signatures to be altered (e.g., Bickle and Baker 1990; Nabelek 1991; Baker and Spiegelman 1995). In the case presented here, fluid infiltration and open-system behavior is recorded as subtle chemical variations within the mineralogy of the pseudomorphs. These pseudomorphs serve to identify fluid infiltration and the episodic influx of B into the rock as well as fluids of different cation activities. In addition, tourmaline growth signifies the timing of this episodic B release. Pseudomorphs record a reaction history and contain evidence of factors that control the evolution of a rock, thus providing the long-lived link between textures and the conditions of formation.

### ACKNOWLEDGMENTS

B.L.D. thanks M.J. Holdaway for introducing her to the bug-infested metamorphic rocks of NW Maine, and for the advice and encouragement over the years. Initial fieldwork was supported by an NSF grant EAR-8306389 to M.J.H. B.L.D. also acknowledges support from NSF EAR-9011034, EAR-9205078, and from the Institute of Geophysics and Planetary Physics at Los Alamos National Lab. Denis Norton is thanked for enlightening B.L.D. on the use of activity diagrams and use of facilities at the University of Arizona during Dutrow's career advancement award, and together with Steve Sorenson, for the activity diagram plotting program. We are grateful to Jack Cheney for providing the Loebner thesis. Mike Holdaway, Charlie Guidotti, and Denis Norton are thanked for their careful and helpful reviews and insights. Texture modeling for this project was supported by NSF grant EAR-9220195 to C.T. Foster. D.J. Henry acknowledges support from NSF grant EAR-9405747.

### REFERENCES CITED

- Ague, J.J. (1994) Mass-transfer during Barrovian metamorphism of pelites, south-central Connecticut. 1. Evidence for changes in composition and volume. *American Journal of Science*, 294, 989–1057.
- Baker, J. and Spiegelman, M. (1995) Modelling an infiltration-driven geochemical front. *Earth and Planetary Science Letters*, 136, 87–96.
- Bassett, R.L. (1980) A critical evaluation of the thermodynamic data for boron ions, ion pairs, complexes, and polyanions in aqueous solutions at 298.15 K and 1 bar. *Geochimica Cosmochimica Acta*, 44, 1151–1160.
- Bickle, M. and Baker, J. (1990) Migration of reaction and isotopic fronts in infiltration zones: assessments of fluid flux in metamorphic terrains. *Earth and Planetary Science Letters*, 98, 1–13.
- Bloodaxe, E.S., Hughes, J.M., Dyar, M.D., Grew, E.S., and Guidotti, C.V. (1999). *Tourmaline: Linking Structure and Chemistry*. *American Mineralogist*, in press.
- Bowers, T.S., Jackson, K.J., and Helgeson, H.C. (1984). *Equilibrium Activity Diagrams for Coexisting Minerals and Aqueous Solutions at Pressures and Temperatures to 5 kb and 600 °C*, 397 p. Springer-Verlag, New York.
- Colucci, M.T., Dyar, M.D., Gregory, R.T., Guidotti, C.V., and Holdaway, M.J. (1991) Hydrogen isotope systematics of biotite-muscovite pairs in high-grade pelitic rocks of southwestern Maine. *Geological Society of America Abstracts with Programs*, 23, 394.
- De Yoreo, J., Lux, D., Guidotti, C., Decker, E., and Osberg, P. (1989) The Acadian thermal history of western Maine. *Journal of Metamorphic Geology*, 7, 169–190.
- Dingwell, D., Pichavant, M., and Holtz, F. (1996) Experimental studies of boron in granitic melts. In *Mineralogical Society of America Reviews in Mineralogy*, 33, 331–386.
- Duke, E.F. (1995) Contrasting scales of element mobility in metamorphic rocks near Harney Peak Granite, Black Hills, South Dakota. *Geological Society of America Bulletin*, 107, 274–285.
- Dutrow, B.L. (1985) Evidence for multiple metamorphic episodes in the Farmington Quadrangle, Maine. p. 115–228. Unpublished Ph.D. Dissertation, Southern Methodist University, Dallas, Texas.
- Dutrow, B. and Foster, C.T., Jr. (1992) Constraints on Metamorphic Fluid from Irreversible Thermodynamic Modeling of Tourmaline Pseudomorph Formation. *Geological Society of America Abstracts with Programs*, 24, A218.
- Dutrow, B.L. and Holdaway, M.J. (1989) Experimental determination of the upper thermal stability of Fe-staurolite + quartz at medium pressures. *Journal of Petrology*, 30, 229–248.
- Dutrow, B.L. and Norton, D.L. (1989) The Effect of Advective Metasomatism of the Interpretation of Isograds in Metapelites. *Transactions, American Geophysical Union*, 70, 1391.
- Dutrow, B.L., Norton, D.L., and Henry, D.J. (1989) Tourmaline-bearing pseudomorphs after staurolite: Boron metasomatism in high grade metapelites. *Geological Society of America Abstracts with Program*, 21, A328.
- Ferry, J.M. (1991) Dehydration and decarbonation reactions as a record of fluid infiltration. In *Mineralogical Society of America Reviews in Mineralogy*, 26, 351–393.
- (1994) Role of fluid-flow in the contact-metamorphism of siliceous dolomitic limestones. *American Mineralogist*, 79, 719–736.
- Fisher, G.W. (1975) The thermodynamics of diffusion controlled metamorphic processes. In A.R. Cooper and A. H. Huer, Eds., *Mass Transport Phenomena in Ceramics*, p. 111–122. Plenum, New York.
- (1977) Nonequilibrium thermodynamics in metamorphism. In D.G. Fraser, Ed., *Thermodynamics in Geology*, p. 381–403. Reidel, Dordrecht, The Netherlands.
- Foster, C.T., Jr. (1977) Mass transfer in sillimanite-bearing pelitic schists near Rangeley, Maine. *American Mineralogist*, 62, 727–746.
- (1981) A thermodynamic model of mineral segregations in the lower sillimanite zone near Rangeley, Maine. *American Mineralogist*, 66, 260–277.
- (1983) Thermodynamic models of biotite pseudomorphs after staurolite. *American Mineralogist*, 68, 389–397.
- (1990) Control of material transport and reaction mechanisms by metastable mineral assemblages: An example involving kyanite, sillimanite, muscovite and quartz. In R.J. Spencer and I-Ming Chou, Eds., *Fluid-Mineral Interactions*, p. 121–132. *Geochemical Special Publication No. 2*. San Antonio, Texas.
- (1993) Seg93: A program to model metamorphic textures. *Geological Society of America Abstracts with Program*, 25, A264.
- Greenwood, H. (1975) Buffering of pore fluids by metamorphic reactions. *American Journal of Science*, 276, 817–840.
- Guidotti, C.V. (1968). Prograde muscovite pseudomorphs after staurolite in the Rangeley-Oquossoc area, Maine. *American Mineralogist*, 53, 1368–1376.
- (1970) Metamorphic petrology, mineralogy, and polymetamorphism in a portion of northwest Maine. In *Guidebook for field trips in the Rangeley Lakes-Dean River Basin region, western Maine*. New England Intercollegiate Geological Conference, 62<sup>nd</sup> Annual Meeting, Field Trip B-2, 1–23.
- (1989). *Metamorphism in Maine*. An overview. *Studies in Maine Geology*. Maine Geological Survey, 3, 1–17. Augusta, Maine.
- Guidotti, C.V. and Holdaway, M.J. (1993). Petrology and field relations of successive metamorphic events in pelites of west-central Maine. In J.T. Cheney and J.C. Hepburn, Eds., *Field Trip Guidebook for the Northeastern United States*, p. L1–L26. Geological Society of America, Boulder, Colorado.
- Guidotti, C.V., Cheney, J.T., Foster, C.T., Hames, W.E., Henry, D.J., Kinner, D.A., and Lux, D.R. (1996) Polymetamorphism in western Maine: mineralogic, petrologic and textural manifestations and regional geologic implications. In M. Van Baalen, Ed., *Guidebook to fieldtrips in northern New Hampshire and adjacent regions of Maine and Vermont*. New England Intercollegiate Geological Conference, 88, 171–202.
- Guidotti, C.V., Berry, H.N. IV, Thomson, J.A., Cheney, J.T., and Hames, W.E. (1998) The geologic envelope enclosing the Sebago Batholith. 1998 GSA Abstracts with Program, Northeastern Section, p. 22.
- Hawthorne, F.C. (1996) Structural mechanisms for light-element variations in tourmaline. *Canadian Mineralogist*, 34, 123–132.
- Helgeson, H.C. (1970) Description and interpretation of phase relations in geochemical processes involving aqueous solutions. *American Journal of Science*, 268, 415–438.
- Henry, D.J. and Dutrow, B.L. (1992) Tourmaline in clastic metasedimentary rocks: an illustration of the petrogenetic potential of tourmaline. *Contributions to Mineralogy and Petrology*, 112, 203–218.
- (1994) Tourmaline in metamorphic rocks: A monitor of boron flux. *Geological Society of America Abstracts with Programs*, 26, A449.

- (1996) Metamorphic tourmaline and its petrologic aspects. In *Mineralogical Society of America Reviews in Mineralogy*, 33, 503–558.
- Holdaway, M.J., Guidotti, C. Novak, J., and Henry, W. (1982) Polymetamorphism in medium- to high-grade pelitic metamorphic rocks, west central Maine. *Bulletin of the Geological Society of America*, 93, 572–584.
- Holdaway, M.J., Dutrow, B.L. and Hinton, R.W. (1988) Devonian and Carboniferous metamorphism in west-central Maine: The muscovite-almandine geobarometer and the staurolite problem revisited. *American Mineralogist*, 73, 20–47.
- Holdaway, M., Mukhopadhyay, B., Dyar, M.D., Guidotti, C. and Dutrow, B. (1997) Garnet-biotite geothermometry revisited: New Margules parameters and a natural specimen data base From Maine. *American Mineralogist*, 82, 582–595.
- Johnson, J.W. and Norton, D. (1985) Theoretical prediction of hydrothermal conditions and chemical equilibria during skarn formation in porphyry copper systems. *Economic Geology*, 80, 1797–1823.
- (1991) Critical phenomena in hydrothermal systems: I. State, thermodynamic, transport, and electrostatic properties of fluid H<sub>2</sub>O in the critical region. *American Journal of Science*, 291, 541–648.
- Johnson, J.W., Oelkers, E.H. and Helgeson, J.C. (1992) SUPCRT92: A software package for calculating the standard molal thermodynamic properties of minerals, gases, aqueous species, and reactions from 1 to 5000 bar and 0 to 1000 °C. *Computers and Geoscience*, 18, 899–947.
- Kohn, M.J. and Valley, J.W. (1994) Oxygen-isotope constraints on metamorphic fluid-flow, Townshend Dam, Vermont, USA. *Geochimica et Cosmochimica Acta*, 58, 5551–5566.
- Kretz, R. (1983) Symbols for rock-forming minerals. *American Mineralogist*, 68, 277–279.
- Kuyunko, N.S., Semonov, Y. Gorevich, V. Kuz' min, V., Topor, N., and Gorbunov (1984) Experimental determination of the thermodynamic properties of tourmaline-drawite. *Geochimica International*, 22, 109–116.
- Leeman, W.P. and Sisson, V.B. (1996) Geochemistry of boron and its implication for crustal and mantle processes. In *Mineralogical Society of America Reviews in Mineralogy*, 33, 645–708.
- Loebner, B.J. (1977) Petrographic Study of Bemis Drill Core Samples from Rangeley Quadrangle, NW, Maine. Unpublished Senior Thesis, Amherst College, Massachusetts.
- London, D. (1986) Magmatic-hydrothermal transition in the Tanco rare-element pegmatite: Evidence from fluid inclusions and phase-equilibrium experiments. *American Mineralogist*, 71, 376–395.
- London, D., Hervig, R., and Morgan, G.B. IV (1988) Melt-vapor solubilities and element partitioning in peraluminous granite-pegmatite systems: Experimental results with Macusani glass at 200 MPa. *Contributions to Mineralogy and Petrology*, 99, 360–373.
- London, D., Morgan, G.B. IV, and Wolf, M. B. (1996) Boron in granitic rocks and their contact aureoles. In *Mineralogical Society of America Reviews in Mineralogy*, 33, 299–330.
- Lynch, G. and Ortega, J. (1997) Hydrothermal alteration and tourmaline-albite equilibria at the Coxheath Porphyry Cu-Mo-Au Deposit, Nova Scotia. *Canadian Mineralogist*, 35, 79–94.
- Morgan, G.B., IV and London, D. (1989) Experimental reactions of amphibolite with boron-bearing aqueous fluids at 200 MPa: implications for tourmaline stability and partial melting in mafic rocks. *Contributions to Mineralogy and Petrology*, 102, 218–297.
- Moench, R.H. and Pankiwskyj, K.A. (1988) Geologic Map of Western Interior Maine. U.S. Geological Survey, Map I-1692.
- Moench, R.H. and Zartman, R.E. (1976) Chronology and styles of multiple deformation, plutonism, and polymetamorphism in the Merrimack synclinorium of western Maine. In R.C. Lyons and A.H. Brownlow, Eds., *Studies in New England Geology*. Geological Society of America Memoir, 146, 203–238.
- Nabelek, P. (1991) Stable isotope monitors. In *Mineralogical Society of America Reviews in Mineralogy*, 26, 395–436.
- Norton, D. (1987) Advective metasomatism. In H.C. Helgeson, Ed., *NATO Advanced Study Institute on Chemical Transport in Metasomatic Processes*, p. 123–132. Reidel, Amsterdam.
- (1988) Metasomatism and permeability. *American Journal of Science*, 288, 604–618.
- Page, L.R. and others (1953) Pegmatite investigations 1942–1945, Black Hills, South Dakota. U.S. Geological Survey Professional Paper 247, 1–228.
- Rice, J. and Ferry, J. (1977) Buffering, infiltration, and the control of intensive variables during metamorphism. In *Mineralogical Society of America Reviews in Mineralogy*, 10, 263–326.
- Shaw, D., Truscott, M, Gray, E., and Middleton, T. (1988) Boron and lithium in high-grade rocks and minerals from the Wawa-Kapusking region, Ontario. *Canadian Journal of Earth Science*, 25, 1485–1502.
- Shearer, C.K., Papike, J., Simon, S., Laul, J., and Christian, R. (1984) Pegmatite/wallrock interactions, Black Hills, South Dakota: Progressive boron metasomatism adjacent to the Tip Top pegmatite. *Geochimica et Cosmochimica Acta*, 48, 2563–2579.
- Shock, E., Helgeson, H., and Sverjensky, D. (1989) Calculation of the thermodynamic and transport properties of aqueous species at high pressures and temperatures: standard partial molal properties of inorganic neutral species. *Geochimica et Cosmochimica Acta*, 53, 2157–2183.
- Slack, J.F. (1996) Tourmaline associations with hydrothermal ore deposits. In *Mineralogical Society of America Reviews in Mineralogy*, 33, 559–663.
- Spear, F. (1993) *Metamorphic Phase Equilibria and Pressure-Temperatures-Time Paths*, 799 p. Mineralogical Society of America Monograph. Washington, D.C.
- Sperlich, R., Giere, R., and Frey, M. (1996) Evolution of compositional polarity and zoning in tourmaline during prograde metamorphism of sedimentary rocks in the Swiss Central Alps. *American Mineralogist*, 81, 1223–1236.

MANUSCRIPT RECEIVED JUNE 25, 1998

MANUSCRIPT ACCEPTED DECEMBER 15, 1998

PAPER HANDLED BY PETER I. NABELEK